



HAL
open science

Assessing influence of diagenetic carbonate dissolution on planktonic foraminiferal Mg/Ca in the southeastern Arabian Sea over the past 450 ka: Comparison between *Globigerinoides ruber* and *Globigerinoides sacculifer*

K. Tachikawa, Sophie Sepulcre, Takashi Toyofuku, Edouard Bard

► To cite this version:

K. Tachikawa, Sophie Sepulcre, Takashi Toyofuku, Edouard Bard. Assessing influence of diagenetic carbonate dissolution on planktonic foraminiferal Mg/Ca in the southeastern Arabian Sea over the past 450 ka: Comparison between *Globigerinoides ruber* and *Globigerinoides sacculifer*. *Geochemistry, Geophysics, Geosystems*, 2008, 9, 10.1029/2007GC001904 . hal-01463327

HAL Id: hal-01463327

<https://hal.science/hal-01463327>

Submitted on 20 Dec 2021

HAL is a multi-disciplinary open access archive for the deposit and dissemination of scientific research documents, whether they are published or not. The documents may come from teaching and research institutions in France or abroad, or from public or private research centers.

L'archive ouverte pluridisciplinaire **HAL**, est destinée au dépôt et à la diffusion de documents scientifiques de niveau recherche, publiés ou non, émanant des établissements d'enseignement et de recherche français ou étrangers, des laboratoires publics ou privés.

Copyright



Assessing influence of diagenetic carbonate dissolution on planktonic foraminiferal Mg/Ca in the southeastern Arabian Sea over the past 450 ka: Comparison between *Globigerinoides ruber* and *Globigerinoides sacculifer*

Kazuyo Tachikawa and Sophie S epulcre

CEREGE, Aix-Marseille Universit e, CNRS, CDF, IRD Europ ole M diterran een de l'Arbois, BP 80, F-13545 Aix en Provence, France (kazuyo@cerege.fr)

Takashi Toyofuku

Research Program for Paleoenvironment, Institute for Research on Earth Evolution, Japan Agency for Marine-Earth Science and Technology, Natsushima-cho 2-15, Yokosuka 237-0061, Japan

Edouard Bard

CEREGE, Aix-Marseille Universit e, CNRS, CDF, IRD Europ ole M diterran een de l'Arbois, BP 80, F-13545 Aix en Provence, France

[1] The influence of supralysoclinal calcite dissolution on the Mg/Ca thermometer over the last 450 ka is assessed using *Globigerinoides ruber* and *Globigerinoides sacculifer* from a core site in the eastern Arabian Sea. The studied site is characterized by precession-cycled paleoproductivity changes that have induced calcite dissolution in the sediments, although the core still contains 40–80% CaCO₃. During high-productivity periods, the narrow-sized test weights of both foraminiferal species tend to decrease with increasing Mn/Ca ratio, indicating corrosive pore water conditions. Scanning electron microscope observations show that *G. sacculifer* maintains a better preserved test ultrastructure than *G. ruber*. Microprobe mapping reveals that Mg-rich bands in *G. ruber* chamber walls are preserved despite reduced Ca content. Assuming that the low test weight and offset in Mg/Ca temperature between *G. sacculifer* and *G. ruber* are exclusively produced by calcite dissolution, the bias in Mg/Ca temperature determination can be estimated at around 1°C, comparable to uncertainty of this thermometry. Despite the evidence for test dissolution, foraminiferal Mg/Ca seems to preserve initial temperature signals under the studied conditions.

Components: 7877 words, 10 figures.

Keywords: supralysoclinal calcite dissolution; foraminiferal Mg/Ca; seawater temperature.

Index Terms: 0473 Biogeosciences: Paleoclimatology and paleoceanography (3344, 4900); 0454 Biogeosciences: Isotopic composition and chemistry (1041, 4870).

Received 16 November 2007; **Revised** 24 January 2008; **Accepted** 15 February 2008; **Published** 26 April 2008.

Tachikawa, K., S. S epulcre, T. Toyofuku, and E. Bard (2008), Assessing influence of diagenetic carbonate dissolution on planktonic foraminiferal Mg/Ca in the southeastern Arabian Sea over the past 450 ka: Comparison between *Globigerinoides ruber* and *Globigerinoides sacculifer*, *Geochem. Geophys. Geosyst.*, 9, Q04037, doi:10.1029/2007GC001904.



1. Introduction

[2] Mg/Ca ratios recorded in calcareous planktonic foraminiferal tests are now considered as an established paleothermometer [Barker *et al.*, 2005]. The most notable advantage of this thermometer is that both seawater temperature and $\delta^{18}\text{O}$ are recorded by the same organisms. It is therefore possible to correct the temperature effect on foraminiferal $\delta^{18}\text{O}$ to estimate local and global salinity variations as well as the timing between changes in local seawater temperature and global ice volume [Mashiotto *et al.*, 1999; Lea *et al.*, 2000; Nürnberg, 2000; Lea, 2004].

[3] One of the serious drawbacks of this paleothermometer is due to the partial dissolution of foraminiferal tests, which may bias the Mg/Ca ratios. This problem arises from the heterogeneous distribution of Mg in tests and the higher solubility of Mg-rich calcite [Russell *et al.*, 1994; Brown and Elderfield, 1996; Lea *et al.*, 2000; Sadekov *et al.*, 2005]. Taking into account the dissolution of tests in bottom waters undersaturated with respect to calcite, calibration equations containing a correction term have been proposed using narrow-ranged foraminiferal test weight [Rosenthal and Lohmann, 2002], carbonate saturation state and water depth [Dekens *et al.*, 2002]. However, the foraminiferal test weight is not only a function of postdepositional dissolution but also calcification conditions such as carbonate ion and nutrient concentrations in surface waters and, more generally, the optimal ecological growth conditions [Bijma *et al.*, 1999; Barker and Elderfield, 2002; de Villiers, 2004; Russell *et al.*, 2004]. Carbonate ion concentration in the past is difficult to constrain and its relationship with water depth may vary with time. To date, there is no perfect method of assessing the influence of test dissolution on foraminiferal Mg/Ca due to contact with undersaturated bottom waters.

[4] Furthermore, calcite dissolution occurs even above the lysocline because of the metabolic release of CO_2 into sediment pore waters during organic matter remineralization. Hence, the organic carbon to calcite flux ratio (rain ratio) has a profound effect on the preservation of carbonates in the deep sea. Indeed, changes in the rain rate have been proposed as a potential factor modulating glacial-interglacial variations in atmospheric CO_2 content [Archer and Maier-Reimer, 1994]. However, while supralysocline calcite dissolution could be a widespread process influencing the global carbon cycle, the effect of diagenetic car-

bonate dissolution on foraminiferal Mg/Ca has not yet been examined.

[5] Here, we present an assessment of the potential influence of calcite dissolution mediated by metabolic respiration on planktonic foraminiferal Mg/Ca in the eastern Arabian Sea for the last 450 ka. We selected *Globigerinoides ruber* (white) and *Globigerinoides sacculifer* (without sac), two spinose mixed layer tropical species frequently used for paleoceanographic studies. The studied core MD90-0963 ($5^{\circ}04'\text{N}$, $74^{\circ}53'\text{E}$, 2446 m water depth) shows a high content of CaCO_3 (40–80%) and is characterized by precession-driven productivity that varies over a sixfold range of magnitude [Bassinot *et al.*, 1994a; Rostek *et al.*, 1994, 1997; Beaufort *et al.*, 1997; Cayre *et al.*, 1999; Schulte *et al.*, 1999; Pailler *et al.*, 2002]. Since the core site is above the present lysocline, and no clear change in lysocline or CCD has been reported over glacial-interglacial timescales during the Neogene in the northwestern Indian Ocean, calcite dissolution at this location is considered to have occurred within the sediment by organic matter remineralization [Schulte and Bard, 2003]. We applied a multiproxy approach including the use of narrow-ranged foraminiferal test weights, foraminiferal Mg/Ca and Mn/Ca obtained by conventional bulk measurements on foraminiferal tests and electron probe microanalysis (EPMA), as well as scanning electron microprobe (SEM) images. Loss of foraminiferal tests during cleaning is also quantified as an indicator of test fragility.

[6] Our results indicate that, despite clear evidence for test dissolution, the foraminiferal Mg/Ca values of both species generally maintain their initial temperature signal within uncertainty of temperature estimate at the studied site, except for *G. ruber* during marine isotope stage (MIS) 11 when test loss exceeded 80%. The influence on foraminiferal Mg/Ca may not only vary with paleoproductivity changes but also with the nature of the sediments such as CaCO_3 content [Jahnke and Jahnke, 2004]. To monitor the potential influence of carbonate dissolution on the Mg/Ca thermometer, we thus strongly recommend the routine analysis of test weights, proportion of test loss during cleaning, foraminiferal Mn/Ca ratio and CaCO_3 content in the bulk sediment.

2. Oceanographic Setting of the Core Site

[7] Core MD90-0963 was collected near the Maldives platform in the eastern Arabian Sea (Figure 1a;

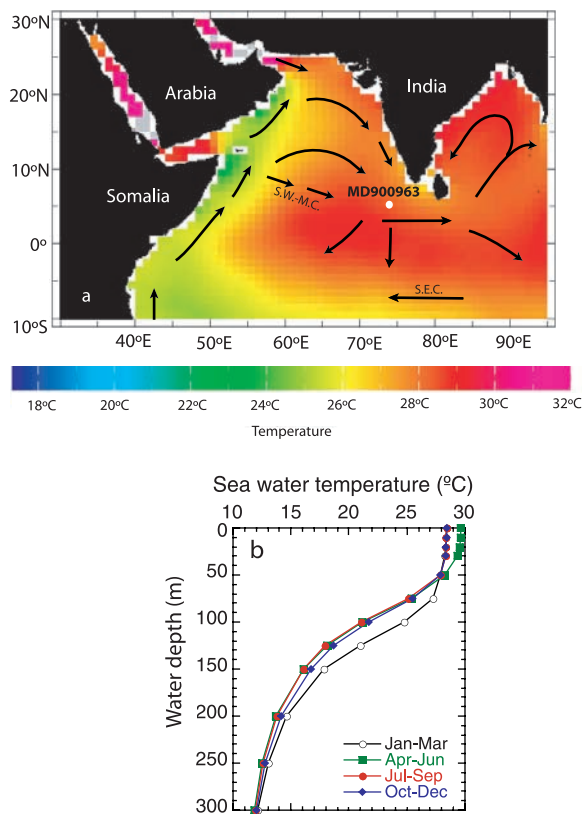


Figure 1. (a) Location map of core site in the Arabian Sea, showing summer (July–September) sea surface temperature and surface ocean currents during the southwest monsoon. SW-MC, southwest monsoon current; SEC, south equatorial current. Adapted by permission from Macmillan Publishers Ltd. [Rostek *et al.*, 1993]. Note that low SST off Somalia and Oman is due to coastal upwelling. (b) Depth profile of modern seasonal seawater temperature at 5.5°N, 73.5°E. Temperature data from WOA98 [Conkright *et al.*, 1998].

5°04'N, 74°53'E, 2446 m water depth). Present-day bottom water at the core site is clearly supersaturated with respect to calcite. The calcite saturation state (Ω) is estimated at 1.10, while the $\Delta\text{CO}_3^{2-} = [\text{CO}_3^{2-}]_{\text{in situ}} - [\text{CO}_3^{2-}]_{\text{calcite saturation}}$ is 6.8 $\mu\text{mol/kg}$ and the pressure-corrected bottom water carbonate ion concentration, $[\text{CO}_3^{2-}]^* = [\text{CO}_3^{2-}] + 20[z(\text{km}) - 4]$ [Broecker and Clark, 2001] is estimated at 105 $\mu\text{mol/kg}$, on the basis of data from GEOSECS station 418 (6.2°N, 64.4°E) and using the CO2SYS program with GEOSECS option [Lewis and Wallace, 2000].

[8] The Arabian Sea is influenced by Indian Monsoon systems. During summer (June–September), southwest monsoon winds lead to intense upwelling along the coasts of Somalia and Oman (Figure 1a). Even though the core site is not directly influenced

by this upwelling, the highest primary productivity (PP) occurs in September, at the end of the southwest summer monsoon. The present-day PP in the Maldives varies between 120 and 300 $\text{C/m}^2/\text{a}$, which is much lower than in the northwestern Arabian Sea where PP ranges between 200 and 600 $\text{gC/m}^2/\text{a}$ [Antoine *et al.*, 1996]. Sea surface temperature (SST) at the studied site varies between 28.0°C (January) and 30.0°C (May), with a mean annual value of 28.7°C (Figure 1b). During the summer, when PP is high, SST is $28.6 \pm 0.4^\circ\text{C}$ and the seawater temperature gradient in the first 30 m is less than 0.1°C (Figure 1b).

3. Samples and Analytical Procedures

[9] Core MD90-0963 has high carbonate contents (40–80%) and the sedimentation rate is estimated at about 5 cm/ka over the last 450 ka [Bassinot *et al.*, 1994a, 1994b]. Precession-cycled marine PP variability at the core location is confirmed by various tracers: foraminiferal and coccolithophore transfer functions, series of biomarkers, organic carbon content, CaCO_3 size index, foraminiferal test fragmentation and authigenic trace element concentrations [Bassinot *et al.*, 1994a; Rostek *et al.*, 1994, 1997; Beaufort *et al.*, 1997; Cayre *et al.*, 1999; Schulte *et al.*, 1999; Pailler *et al.*, 2002]. According to foraminiferal and coccolithophore assemblages, reconstructed PP ranges from 70 to 390 $\text{gC/m}^2/\text{a}$ over the last 450 ka [Beaufort *et al.*, 1997; Cayre *et al.*, 1999]. Foraminiferal samples for this study were selected from sediment depth intervals corresponding to high or low PP periods, taking into account all the available PP indicators (Figure 2). In the following, foraminiferal tests from these intervals are referred as “high PP” and “low PP” samples.

[10] More than 50 tests of *G. ruber* and *G. sacculifer* were hand picked from 212 to 300 μm and 355–425 μm size fractions, respectively, following [Rosenthal and Lohmann, 2002]. Then, tests were briefly cleaned by ultrasonication taking special care to minimize fragmentation. After drying, 50 tests were weighed using a Sartorius microbalance (Sartorius MC5) at CEREGE to obtain mean individual test weights.

[11] The weighed tests were gently crushed between two glass plates and further cleaned using the multistep “Mg method” [Barker *et al.*, 2003]. As we are interested here in foraminiferal Mn/Ca changes as an indicator of pore water chemistry, we left out a reductive step. In fact, a recent study

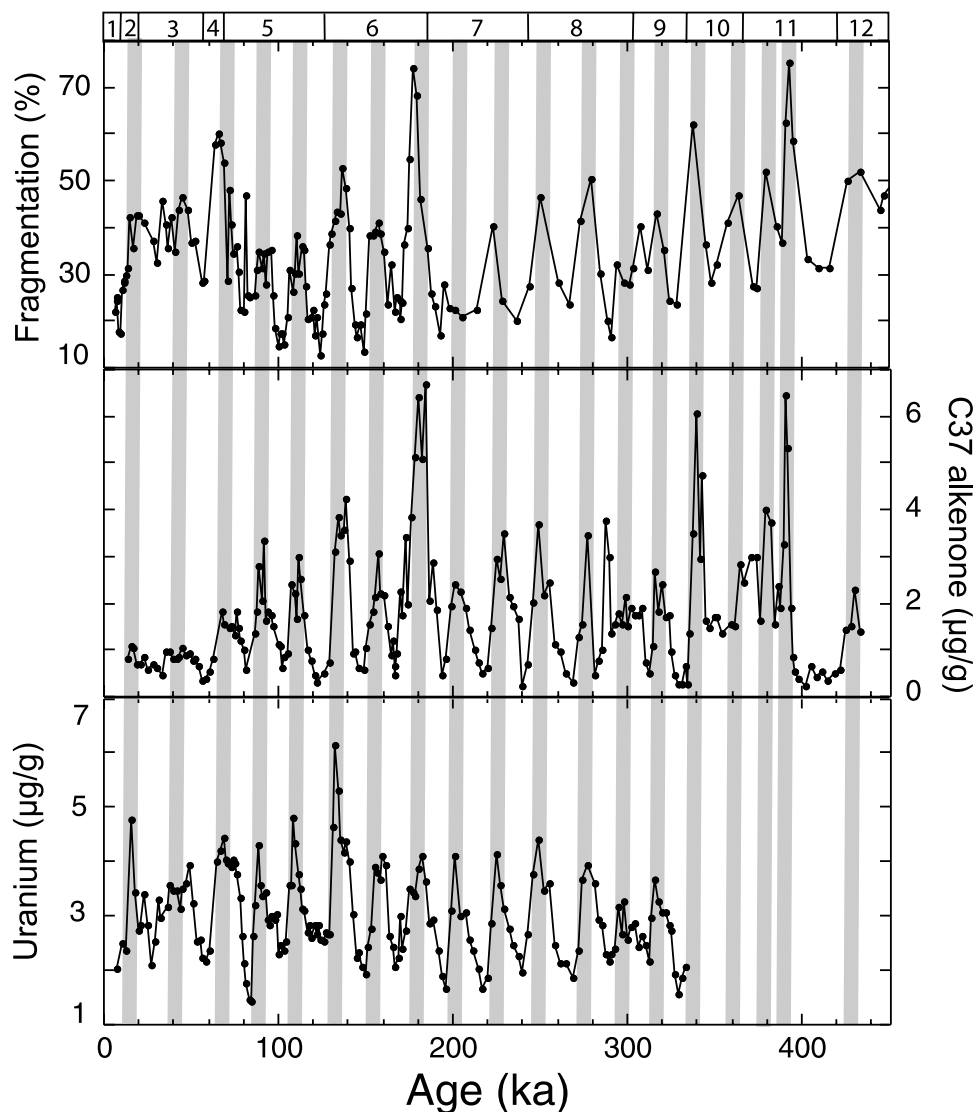


Figure 2. (top) Foraminiferal fragmentation index, (middle) total alkenone concentration, and (bottom) uranium concentration in bulk sediment as indicators of precession-cycled productivity changes observed in core MD90-0963 over the last 450 ka. High-productivity periods are indicated with gray bands. Data from *Bassinot et al.* [1994b], *Pailler et al.* [2002], and F. Rostek (unpublished data, 1998). Chronostratigraphy is based on *Bassinot et al.* [1994a]. Marine isotope stages are indicated in Figure 2 (top).

showed that high foraminiferal Mn/Ca does not influence foraminiferal Mg/Ca at a core site close to the present location ($2^{\circ}40'N$, $78^{\circ}00'E$) [*Saraswat et al.*, 2006]. The cleaned test fragments were dissolved in 0.075 M HNO_3 , and the solutions were centrifuged to remove particulate impurities. The final solutions were diluted with distilled 2% HNO_3 and analyzed for Mg/Ca and Mn/Ca by ICP-OES (Jobin Yvon Ultima C) at CEREGE using the intensity calibration method [*de Villiers et al.*, 2002]. The accuracy of our measurements was confirmed by international calibration [*Rosenthal et al.*, 2004]. The mean external reproducibility and

accuracy of Mg/Ca are better than 0.5%. Mg/Ca data with Fe/Mg more than 0.1 mol/mol were discarded because of potential clay contamination. To estimate test fragility, we calculated the proportion of test loss during cleaning using Ca concentrations obtained by ICP-OES measurements, assuming that the weighed tests were composed of pure $CaCO_3$.

[12] In addition to the batch analyses, microscale measurements were carried out using EPMA (JEOL JXA-8900RL) at JAMSTEC for “high PP” and “low PP” *G. ruber* specimens from

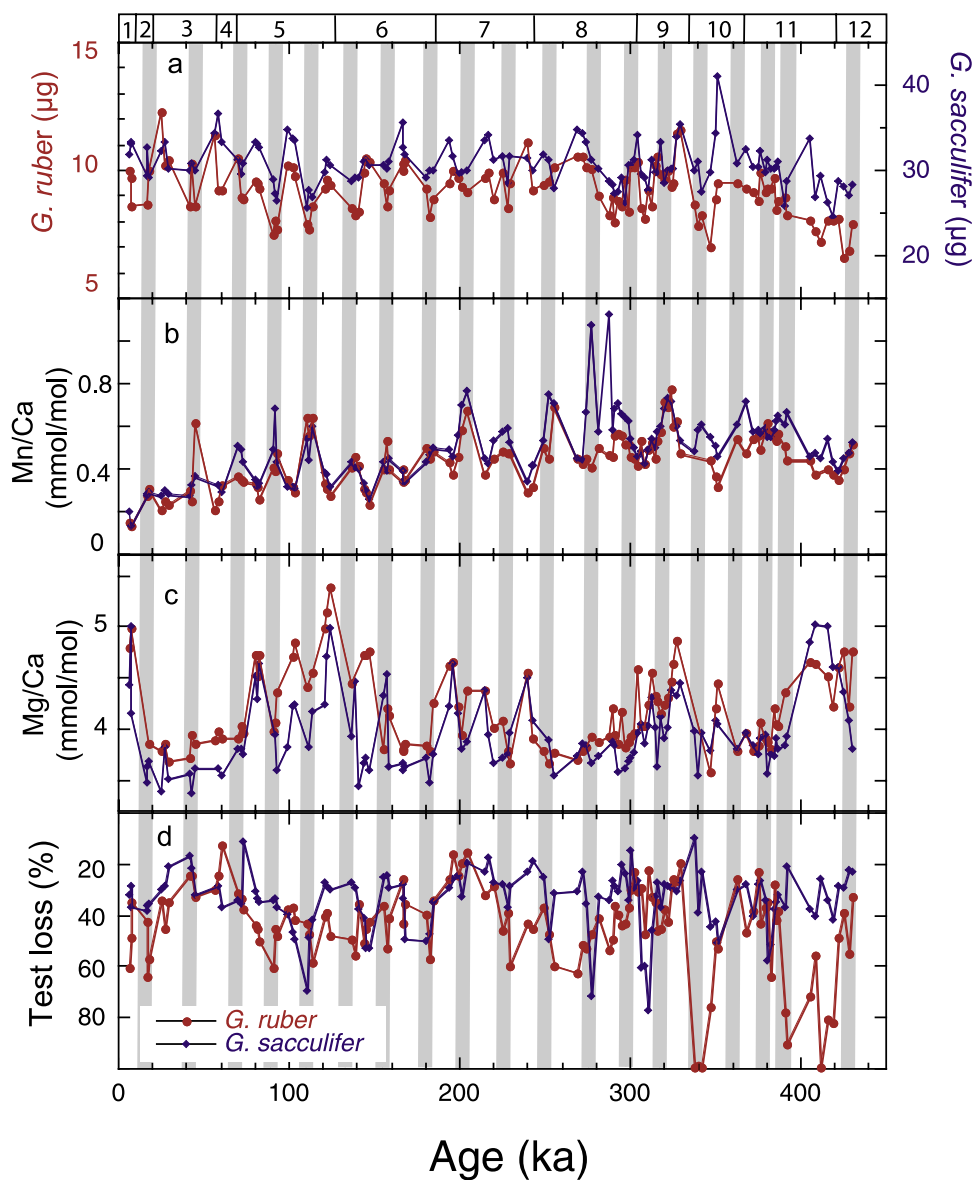


Figure 3. Test weights and chemistry of *G. ruber* (212–300 μm) and *G. sacculifer* (355–425 μm) over the last 450 ka, along with test loss during cleaning by “Mg method.” (a) Individual test weights, (b) foraminiferal Mn/Ca, (c) foraminiferal Mg/Ca, and (d) proportion of test loss during cleaning. Results for *G. ruber* and *G. sacculifer* are indicated in red and blue, respectively. Marine isotope stages and high PP periods are the same as in Figure 2.

MIS 5. Prior to analysis, the specimens were embedded in epoxy resin to fill the chamber cavities and polished to expose the required cross section of the tests. Then, the surface was coated with a 20-nm-thick carbon film by vacuum evaporation. Mg and Ca measurements were performed at an accelerating voltage of 15 kV and a beam current of 300 nA with a dwell time of 50 ms. The electron probe was focused on the measurement surface ($>1 \mu\text{m}$). The resolution of each pixel is $0.5 \mu\text{m}$ by $0.5 \mu\text{m}$ on the elemental map. Homogeneous coral powder JcP-1 was used as a stan-

dard for Ca and Mg quantification [Okai *et al.*, 2001]. We estimated the reproducibility of EPMA measurements by randomly selecting 100 points characterized by similar Mg/Ca values for the sample of this study. The obtained reproducibility (1σ) is 13.4% for each pixel, which corresponds to a relative standard deviation of 1.34%.

[13] Test ultrastructure (state of spine, spine bases, ridges, interpore area and pores [Dittert and Henrich, 2000]) was examined by SEM. Three individual specimens of both species from the

“high PP” and “low PP” samples from MIS 1, 5, 6, 10 and 11 were glued onto a stub, gold-coated and observed using a JEOL JSM6320F instrument (3 kV accelerating voltage) at CRMC2 (Aix-Marseille II University, France).

4. Results

4.1. *Globigerinoides ruber* and *Globigerinoides sacculifer* Test Weights and Elemental Ratios Over the Last 450 ka

[14] Core top test weights are 10.0 μg and 31.9 μg for *G. ruber* and *G. sacculifer*, respectively (Figure 3a). The core top *G. sacculifer* weight is consistent with the value expected from the correlation between pressure-corrected bottom water carbonate ion concentration, $[\text{CO}_3^{2-}]^*$, and test weight established with a large data set including samples from the Indian Ocean [Rosenthal et al., 2000; Broecker and Clark, 2001; Rosenthal and Lohmann, 2002; de Villiers, 2003]. In contrast, the core top *G. ruber* weight is about 3 μg heavier than the value expected from the test weight–carbonate ion relationship based on the equatorial Atlantic data [Rosenthal and Lohmann, 2002]. Both species show a decrease in test weight in relation to productivity over the last 350 ka, whereas no clear trend with productivity is observed between 450 ka and 350 ka. For the whole studied period, there is no trend in relation with glacial-interglacial cycles. *G. ruber* weight ranges between 7.0 and 12.3 μg for the last 350 ka, with a decrease of 1–2 μg for the “high PP” samples, while, from 450 ka to 350 ka, it increases from 6.6 to 9.5 μg . The weight of *G. sacculifer* ranges between 25.6 μg and 36.7 μg over the last 350 ka, with a similar or slightly weaker trend with PP compared to *G. ruber*. From 450 ka to 350 ka, the weight of *G. sacculifer* increases from 24.6 to 34.3 μg , apart from a positive spike of 41.0 μg at 351 ka (Figure 3a).

[15] Mn/Ca ratios for *G. ruber* and *G. sacculifer* generally increase from the core top down into the core from 0.1 to 0.6 mmol/mol (Figure 3b). Superimposed on this long-term trend, the Mn/Ca of both species clearly increases by 0.1 to 0.2 mmol/mol in the “high PP” samples. Since the Mn/Ca of foraminifera devoid of Mn oxide coatings is of the order of 0.1–0.2 mmol/mol, the observed Mn enrichment is due to Mn mobilization related to pore water chemistry. No clear trend is observed on the scale of glacial-interglacial variations.

[16] Mg/Ca curves for *G. ruber* and *G. sacculifer* show very similar glacial-interglacial cycles over the last 450 ka (Figure 3c). Mg/Ca of *G. ruber* is systematically higher than the value for *G. sacculifer*, except for early MIS 11. Mg/Ca for *G. ruber* ranges between 3.58 and 5.38 mmol/mol, whereas for *G. sacculifer*, it ranges between 3.37 and 5.03 mmol/mol. There is no systematic relationship between Mg/Ca and PP. For instance, from MIS 4/5 transition to MIS 2, Mg/Ca does not decrease in relation to PP (Figure 3c). Consequently, there is no positive correlation between Mg/Ca and Mn/Ca. This implies that Mn oxide coatings do not form an important contaminant phase at the studied site.

[17] For the whole studied core record, we estimate $44 \pm 17\%$ and $34 \pm 12\%$ of *G. ruber* and *G. sacculifer* tests are lost because of cleaning, respectively (Figure 3d). The proportion of test loss does not vary in relation to precession-related or glacial-interglacial cycles. On the contrary, foraminiferal test loss increases down core, in particular for *G. ruber* at the end of MIS 10 and MIS 11 where it exceeds 80%.

4.2. Microscale Analyses of Selected *Globigerinoides ruber* and *Globigerinoides sacculifer* Tests

[18] Test ultrastructure degradation is an indicator of carbonate dissolution that can be evaluated by the state of the spine, spine bases, ridges, interpore areas and pores [Dittert and Henrich, 2000]. With advancing dissolution, the spines disappear, spine bases and ridges are reduced, while pores are broadened and interpore cracks appear. We systematically examined the upper chambers of selected foraminifera specimens by SEM. For *G. ruber*, spines are always absent even in the core top material (Figure 4a). For core top *G. ruber*, spine bases are slightly denuded but pores are round and the interpore area is smooth (Figure 4a). “Low PP” *G. ruber* from MIS 6 (145 ka) has slightly denuded spine bases and ridges, but pores are round and the interpore area remains smooth (Figure 4b). By contrast, “high PP” specimens from MIS 11 (393 ka) are characterized by signs of dissolution with reduced spine bases, and broadened and funnel-like pores (Figure 4c). Similar dissolution effects are clearly observed for “high PP” *G. ruber* from MIS 6 (140 ka), but not for the “low PP” specimens, even from the lower part of the core (MIS 10, 350 ka) (not shown in Figure 4). In general, *G. sacculifer* specimens show better preservation compared to *G. ruber*, with intact

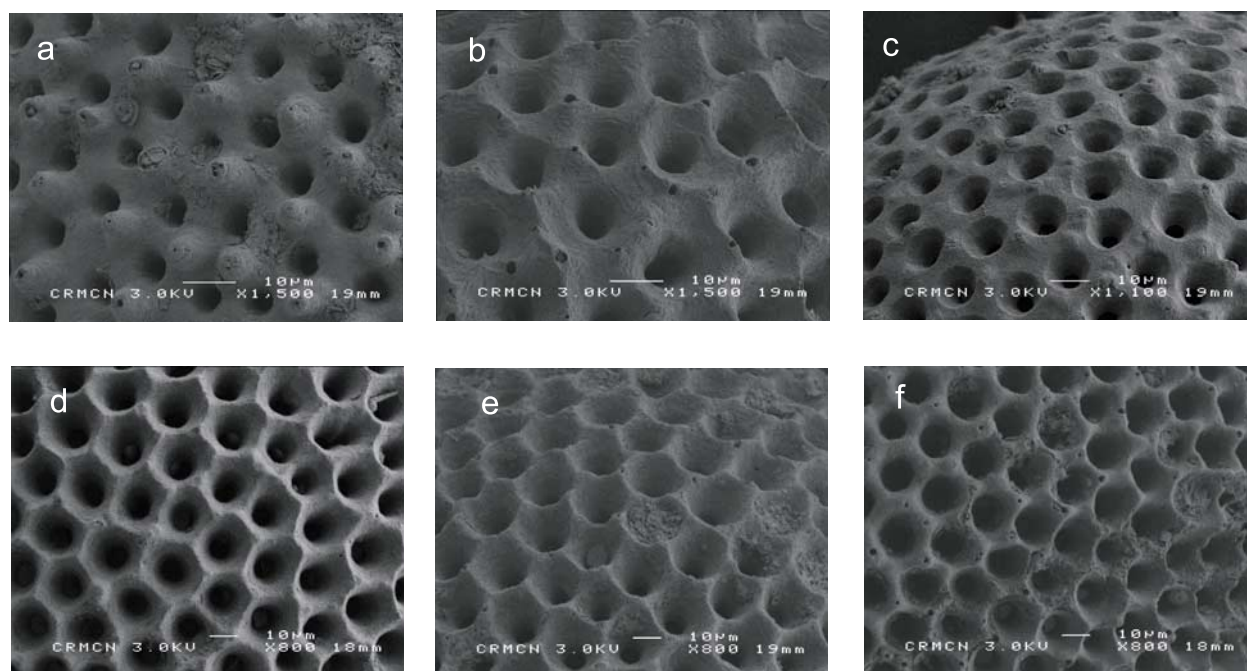


Figure 4. SEM micrographs of *G. ruber* and *G. sacculifer* with detailed images of wall textures. (a) *G. ruber* from core top ($\times 1500$). (b) *G. ruber* from low-productivity period (145 ka, $\times 1500$). (c) *G. ruber* from high-productivity period (393 ka, $\times 1100$). (d) *G. sacculifer* from low-productivity period (81 ka, $\times 800$). (e) *G. sacculifer* from high-productivity period (100 ka, $\times 800$). (f) *G. sacculifer* from low-productivity period (350 ka, $\times 800$).

spine bases and ridges, and round pores for both low- and high-productivity periods of MIS 5 (81 ka and 100 ka; Figures 4d and 4e) and MIS 10 (350 ka; Figure 4f). One noticeable difference related to PP is that spines are observed inside chambers of “low PP” specimens, while they have disappeared from the “high PP” samples (not shown in Figure 4).

[19] We used EPMA to examine the influence of dissolution on microscale elemental distribution in selected *G. ruber* specimens (Figures 5–7). Ca distribution in *G. ruber* chamber sections is clearly different between periods of low PP (MIS 5c, 102 ka) and high PP (MIS 5d, 112 ka). For the “low PP” sample, Ca concentrations are fairly homogeneous and the chamber edge is sharp (Figures 5a and 5b). In contrast, the Ca distribution in the “high PP” test is rather heterogeneous with more area exhibiting lower Ca concentrations (Figure 5c). The edges become irregular, while pores are broader and deeper, leading to reduced test density (Figures 5c and 5d). This observation is consistent with lower test weight for the “high PP” samples (Figure 3a). No systematic trend is observed for test wall thickness under different PP conditions.

[20] Elemental mapping of the chamber sections indicates generally higher Mg/Ca ratios for tests

from warm MIS 5c (lower productivity period, Figure 6a) compared with cool MIS 5d (higher-productivity period, Figure 6b), which is consistent with the bulk analysis (Figures 3c, 6a, and 6b). Mg distribution in the chamber sections is heterogeneous, with Mg-rich bands in both “high PP” and “low PP” samples. The Mg-rich bands are thought to be formed by the vital effects of symbiont-bearing species [Sadekov *et al.*, 2005]. In the present study, we examined the resistance of the bands to artificial oxidation because the bands are related to organic membranes [Hemleben *et al.*, 1988; Eggins *et al.*, 2003]: the “low PP” test (MIS 5c, 102 ka) was gently crushed between two glass plates, then the fragments were treated with 1:1 mixture of 0.1M NaOH and 8% H₂O₂ at 50°C for 18 h. Cleaned fragments were dried, embedded in epoxy resin and treated as described above. Results indicates that the Mg-rich bands persist after the oxidation (Figures 7a–7d), indicating that the Mg enrichment related to intercrystalline organic matter is resistant to oxidation.

5. Discussion

[21] For the “high PP” samples, test weights of both species tend to decrease with increasing for-

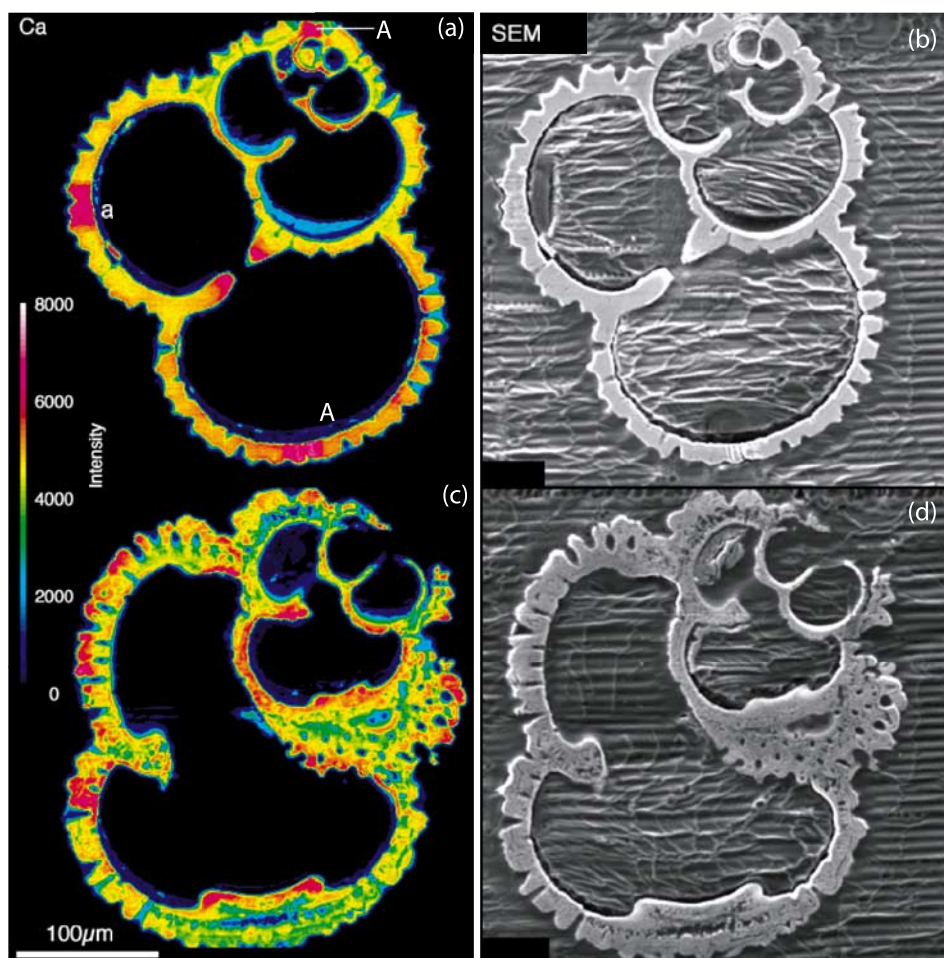


Figure 5. (a and b) *G. ruber* from a low-productivity sediment interval corresponding to cool MIS 5c (102 ka). (c and d) *G. ruber* from a high-productivity sediment interval corresponding to warm MIS 5d (112 ka). Calcium distribution in *G. ruber* chamber wall cross sections obtained by EPMA measurements (Figures 5a and 5c) are shown together with SEM images (Figures 5b and 5d).

miniferal Mn/Ca, indicating a decrease in pH and redox potential (Eh) of pore waters due to metabolic CO₂. Foraminiferal Mg/Ca shows well-characterized glacial-interglacial variability, which overlaps the precession cycles. This makes it difficult to distinguish the effects of temperature from dissolution. SEM analyses indicate that *G. sacculifer* is more dissolution-resistant than *G. ruber*. EPMA measurements show that Mg-rich bands in *G. ruber* tests are preserved in spite of the Ca depletion in the partially dissolved tests. No systematic trend is observed for wall thickness of the “high PP” and “low PP” tests. These microscale observations suggest that calcite dissolution does not fractionate ontogenically distinct test parts.

[22] In the following, we first examine the relationship between foraminiferal test weights and

possible changes in carbonate ion concentration. Then, we quantify the potential Mg/Ca temperature bias due to calcite dissolution assuming that (1) test weight changes are exclusively produced by calcite dissolution and (2) the dissolution correction established for bottom water is valid for supralysocline dissolution. Finally, we compare Mg/Ca between *G. ruber* and *G. sacculifer* to evaluate the temperature bias, since there are distinct differences in dissolution resistance between the two species. Although SST based on alkenone unsaturation index is available for core MD90-0963 [Rostek *et al.*, 1993], we do not undertake here any comparison between proxies. This is because the offset between the SST proxies cannot be interpreted by foraminiferal dissolution alone and it would be necessary to evaluate the impact of seasonality, calcification depth, bioturbation and changes in

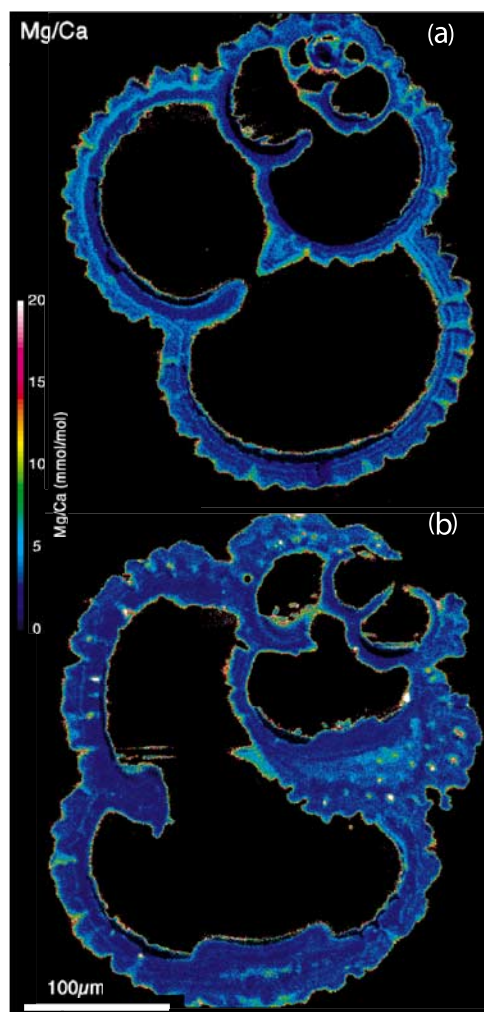


Figure 6. (a and b) Mg/Ca ratios in *G. ruber* chamber wall cross sections of the same specimen shown in Figures 5a and 5c obtained by EPMA.

alkenone producers with time [Muller et al., 1997; Bard, 2001a, 2001b; Andruleit et al., 2003].

5.1. *Globigerinoides ruber* and *Globigerinoides sacculifer* Test Weights and Possible Changes in Carbonate Saturation State

[23] Concomitant changes in test weight and foraminiferal Mn/Ca of the two species (Figures 3a and 3b) indicate that the test weight changes are at least partly controlled by calcite dissolution in pore water. If *G. ruber* and *G. sacculifer* test weights were exclusively controlled by postmortem dissolution, the weights of two species would be strongly correlated with each other. Indeed, the weights of the two species from core MD90-0963

show a significant positive correlation ($R = 0.55$, Figure 8). We thus estimate the past calcite saturation state, ΔCO_3^{2-} , using the test weights provided that the previously established weight-carbonate ion relationship can be applicable to pore water $[\text{CO}_3^{2-}]^*$, and $[\text{CO}_3^{2-}]^*$ calcite saturation is constant with time. Using *G. sacculifer* test weights from core MD90-0963 and the slope of the linear regression between test weight and $[\text{CO}_3^{2-}]^*$, $\Delta\text{wt}_{\text{sacculifer}}/\Delta[\text{CO}_3^{2-}]^* = 0.31$ ($\mu\text{g}/\mu\text{mol.kg}^{-1}$) [Rosenthal et al., 2000; Broecker and Clark, 2001; Rosenthal and Lohmann, 2002; de Villiers, 2003], we obtain ΔCO_3^{2-} for the last 450 ka ranging from -16.7 $\mu\text{mol/kg}$ to 36.2 $\mu\text{mol/kg}$ (Figure 8). The ΔCO_3^{2-} estimation from *G. ruber* test weight is less straightforward because the relationship $\Delta\text{wt}_{\text{ruber}}/\Delta[\text{CO}_3^{2-}]^*$ established for the equatorial Atlantic [Rosenthal and Lohmann, 2002] does not fit the data from the Arabian Sea (section 4.1). We thus deduce $\Delta\text{wt}_{\text{ruber}}/\Delta[\text{CO}_3^{2-}]^*$ from the regression between *G. ruber* and *G. sacculifer* test weights. Considering $\Delta\text{wt}_{\text{sacculifer}}/\Delta\text{wt}_{\text{ruber}} = 1.4$ $\mu\text{g}/\mu\text{g}$ (Figure 8), the estimated $\Delta\text{wt}_{\text{ruber}}/\Delta[\text{CO}_3^{2-}]^* = \Delta\text{wt}_{\text{sacculifer}}/\Delta[\text{CO}_3^{2-}]^*/(\Delta\text{wt}_{\text{sacculifer}}/\Delta\text{wt}_{\text{ruber}}) = 0.31/1.4 = 0.22$ ($\mu\text{g}/\mu\text{mol.kg}^{-1}$). Consequently, *G. ruber* weight variation yields ΔCO_3^{2-} values ranging from -8.7 $\mu\text{mol/kg}$ to 17.1 $\mu\text{mol/kg}$ for the last 450 ka (Figure 8). These ΔCO_3^{2-} values will be used to quantify possible bias of SST estimates in the following section.

5.2. Evaluation of Possible SST Bias Using Test Weight Variations

[24] The possible bias of Mg/Ca temperature $\Delta(T_{\text{corr-not,corr}})$ due to dissolution can be quantified using Mg/Ca calibration equations that take account of test weights [Rosenthal and Lohmann, 2002] and calcite saturation state ΔCO_3^{2-} [Dekens et al., 2002] as correction terms. $\Delta(T_{\text{corr-not,corr}})$ values are calculated by subtracting the uncorrected temperature using core top weight or modern ΔCO_3^{2-} for the whole record from the corrected temperature using weight or ΔCO_3^{2-} at each interval. However, it is important to bear in mind that the dissolution-correction terms may introduce artifacts if test weights are not predominantly controlled by calcite dissolution, in which case the past ΔCO_3^{2-} values are incorrectly estimated.

[25] Seawater temperatures estimated from core top foraminiferal Mg/Ca values using the calibration equation of Rosenthal and Lohmann [2002] are 26.3°C and 28.1°C for *G. ruber* and *G. sacculifer*,

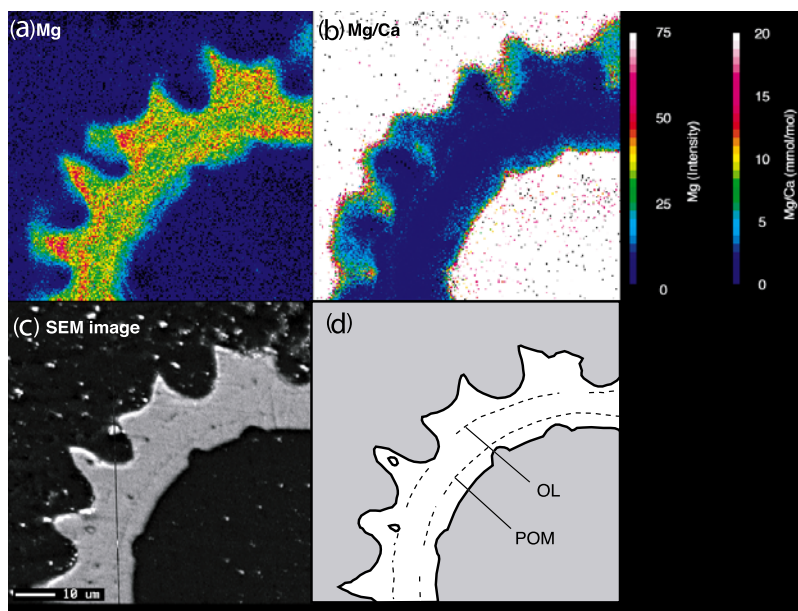


Figure 7. Test fragment (MIS 5c) treated with oxidative cleaning to examine the resistance of high Mg bands (see text for explanation): (a) Mg distribution, (b) Mg/Ca ratios, (c) SEM image, and (d) schematic diagram of test structure. Relatively scattered dark spots in the test wall on the SEM image (Figure 7c) are identified as the outer organic layer (OL) and primary organic membrane (POM) (Figure 7d) [Bé *et al.*, 1980].

respectively. The Mg/Ca temperature for *G. sacculifer* is close to the present mean summer SST of $28.6 \pm 0.4^\circ\text{C}$ (section 2), whereas *G. ruber* yields a significantly lower result. The *G. ruber* Mg/Ca temperatures are systematically lower than those obtained for *G. sacculifer* values for the whole record, with a mean offset of 2°C . *G. ruber* is considered to be the best recorder of sea surface temperature (SST), whereas *G. sacculifer* may show some slight influence from subsurface water (20–30 m) [Hemleben *et al.*, 1988; Dekens *et al.*, 2002]. Both species are warm surface dwellers and expected to occur during similar periods [Hemleben *et al.*, 1988; Kawahata *et al.*, 2002]. Taking into account the present seasonal surface water temperature and vertical temperature profiles at the studied site as well as calcification depths of the species (section 2, Figure 1b), Mg/Ca temperatures for both species should be close to each other at least in the core top samples. The observed temperature offset suggests that the calibration equation is not appropriate for *G. ruber* at the studied site. Estimated $\Delta(T_{\text{corr-not.corr}})$ ranges from -1.5°C to 2.5°C for *G. ruber*, and from -0.6 to 0.9°C for *G. sacculifer* during the last 350 ka when precession-cycled PP changes are clearly observed (Figure 9a). The range of $\Delta(T_{\text{corr-not.corr}})$ for *G. sacculifer* is of the same order as the uncertainty of about 1°C in the foraminiferal Mg/Ca temperature [Barker *et al.*, 2005]. *G. ruber* shows a larger range of $\Delta(T_{\text{corr-not.corr}})$, in

particular for MIS 12 and early MIS 11 when the test loss during cleaning exceeds 80% (Figure 3d). However, $\Delta(T_{\text{corr-not.corr}})$ results for *G. ruber* should be interpreted with caution because the calibration equation is probably not suitable for this species at the studied site.

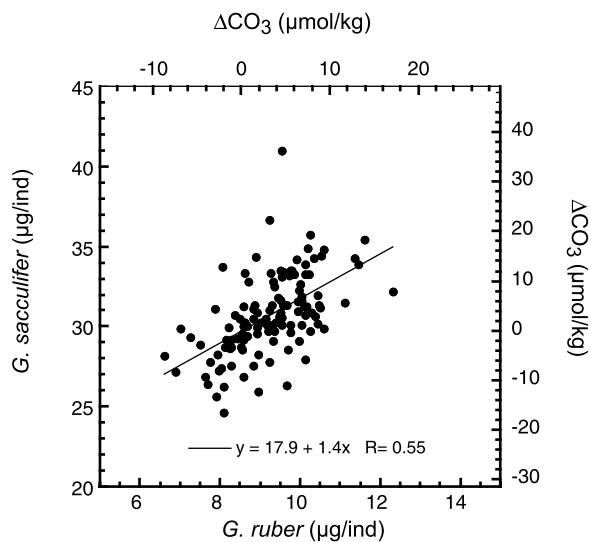


Figure 8. Relationship between individual test weights of *G. ruber* (212–300 μm) and *G. sacculifer* (355–425 μm) over the last 450 ka and estimated variability of past calcite saturation state (ΔCO_3^-) based on *G. ruber* weight (top x axis) and *G. sacculifer* weight (left y axis). See text for explanation.

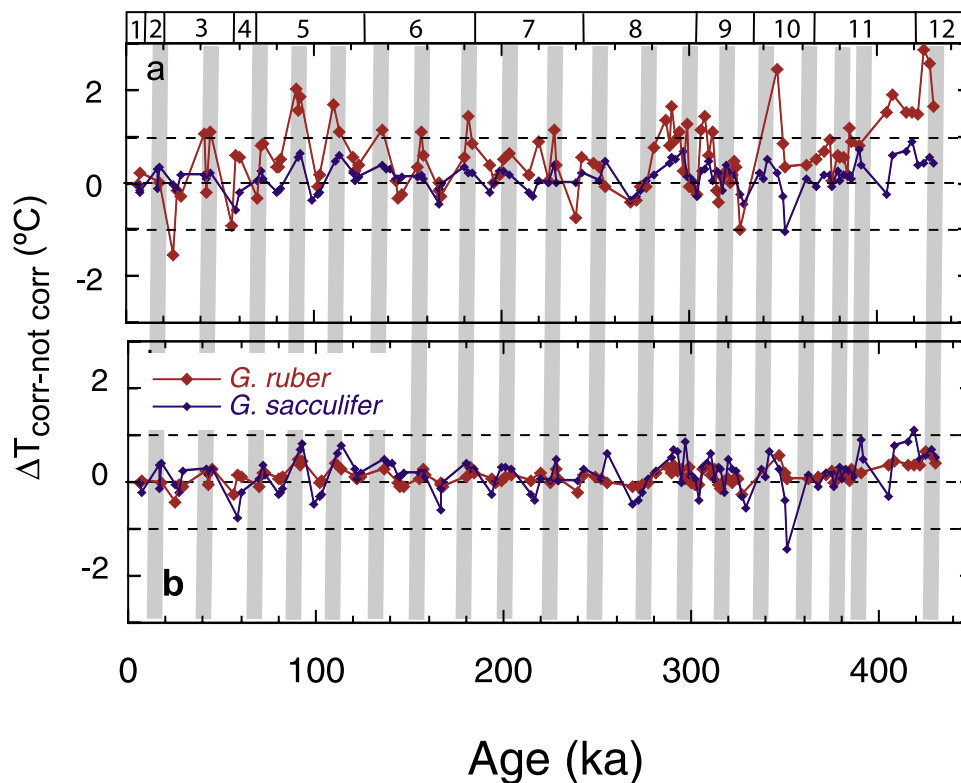


Figure 9. Possible Mg/Ca temperature bias $\Delta(T_{\text{corr-not,corr}})$ due to foraminiferal dissolution over the last 450 ka. (a) Temperature calculated with calibration equations of *Rosenthal and Lohmann* [2002] using foraminiferal weights as a correction term: $(\text{Mg}/\text{Ca})_{\text{ruber}} = (0.025\text{wt} + 0.11)\exp(0.095T)$, $(\text{Mg}/\text{Ca})_{\text{sacc}} = (0.0032\text{wt} + 0.181)\exp(0.095T)$. Corrected temperature is calculated using test weight at each depth interval, whereas uncorrected temperature is calculated using core top weight for the whole record. (b) Temperature calculated with calibration equations of *Dekens et al.* [2002] using ΔCO_3^{2-} as a correction term (see text and Figure 8 for details): $(\text{Mg}/\text{Ca})_{\text{ruber}} = 0.33\exp[0.09(T + 0.042(\Delta\text{CO}_3^{2-}))]$, $(\text{Mg}/\text{Ca})_{\text{sacc}} = 0.31\exp[0.084(T + 0.048(\Delta\text{CO}_3^{2-}))]$. Corrected temperature is calculated using estimated ΔCO_3^{2-} at each interval, whereas uncorrected temperature is calculated using the modern ΔCO_3^{2-} for the whole record. Foraminiferal Mg/Ca values of core MD90-0963 were obtained by “Mg cleaning,” which does not involve a reductive step (section 3), whereas the calibration equations were established using Cd cleaning with the reductive step. Hence, we reduce our foraminiferal Mg/Ca values by 8% to correct for bias related to the different cleaning methods [*Rosenthal et al.*, 2004]. *G. ruber* and *G. sacculifer* results are indicated in red and blue, respectively. Horizontal dashed lines indicate no temperature bias and a $\Delta(T_{\text{corr-not,corr}})$ range of $\pm 1^\circ\text{C}$. Marine isotope stages and high PP periods are the same as in Figure 2.

[26] An alternative estimation of $\Delta(T_{\text{corr-not,corr}})$ is based on the calibration equations of *Dekens et al.* [2002] with ΔCO_3^{2-} as a correction term. Seawater temperatures estimated from core top Mg/Ca values are 28.5°C and 30.3°C for *G. ruber* and *G. sacculifer*, respectively. In this case, the Mg/Ca temperature from *G. sacculifer* is too high. It is noteworthy that the *G. sacculifer* calibration proposed by *Dekens et al.* [2002] was established using the 250–355 μm size fraction, which is finer than that used in this study (355–425 μm). For the whole record, the Mg/Ca temperature from *G. sacculifer* is higher than from *G. ruber* (mean offset of 2°C), indicating the calibration equation might be inap-

propriate for *G. sacculifer*. The estimated $\Delta(T_{\text{corr-not,corr}})$ ranges are from -0.4°C to 0.6°C , and from -0.7°C to 0.9°C during the last 450 ka for *G. ruber* and *G. sacculifer*, respectively (Figure 9b).

[27] A final assessment of the influence of calcite dissolution is based on comparing Mg/Ca temperatures between *G. ruber* and *G. sacculifer*. Since SEM observations indicate that *G. sacculifer* tests are better preserved than *G. ruber* tests, the difference in Mg/Ca temperature between these two species, $\Delta(\text{Mg}/\text{Ca}-T)_{\text{ruber-sacc}}$, could provide some insight into the influence of calcite dissolution without introducing any correction term into the calibration equation. However, the magnitude of $\Delta(\text{Mg}/\text{Ca}-T)_{\text{ruber-sacc}}$

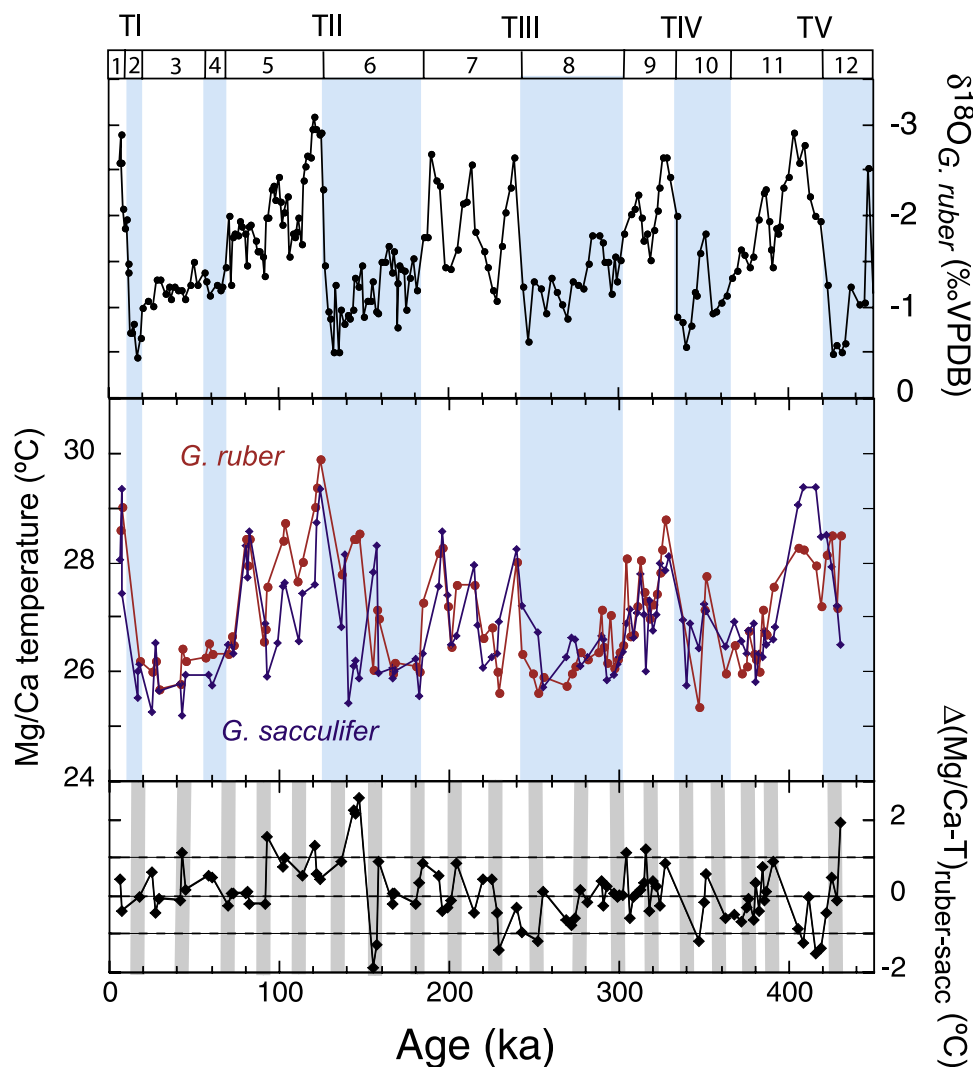


Figure 10. Comparison of *G. ruber* and *G. sacculifer* Mg/Ca temperatures over the last 450 ka together with *G. ruber* $\delta^{18}\text{O}$ of core MD90-0963 [Bassinot et al., 1994a]. *G. ruber* and *G. sacculifer* Mg/Ca values are converted into seawater temperatures using the calibration equations of Dekens et al. [2002] and Rosenthal and Lohmann [2002], respectively, without any dissolution correction. The difference between *G. ruber* and *G. sacculifer* Mg/Ca temperatures, $\Delta(\text{Mg}/\text{Ca}-T)_{\text{ruber-sacc}}$, is indicated at the bottom. Horizontal dashed lines show no temperature bias and $\Delta(\text{Mg}/\text{Ca}-T)_{\text{ruber-sacc}}$ range of $\pm 1^\circ\text{C}$. Marine isotope stages and high PP periods are the same as in Figure 2. Blue bars indicate glacial periods.

may vary with relative changes of calcification depths for the two species. Therefore, we focus here on $\Delta(\text{Mg}/\text{Ca}-T)_{\text{ruber-sacc}}$ variations in relation to PP changes rather than examining absolute $\Delta(\text{Mg}/\text{Ca}-T)_{\text{ruber-sacc}}$ values. Mg/Ca temperatures for *G. ruber* and *G. sacculifer* are respectively calculated using the calibration equations of Dekens et al. [2002] and Rosenthal and Lohmann [2002], because these calibrations yield core top temperatures consistent with modern SSTs.

[28] The Mg/Ca temperatures estimated from the two species generally show very similar glacial-

interglacial cycles as well as almost the same absolute temperature values (Figure 10). We should point out that the foraminiferal Mg/Ca temperature changes of both species are strikingly similar to the $\delta^{18}\text{O}$ variations of *G. ruber* [Bassinot et al., 1994a], which is partly influenced by local seawater temperature. The amplitude of glacial-interglacial temperature changes is 3°C to 4°C for the last five terminations, consistent with SST records covering the same periods from the western and eastern tropical Pacific where past productivity was not influenced by precession cycles [Lea et al., 2000]. From the Holocene to MIS 5, Mg/Ca temper-



atures from *G. ruber* are equivalent or slightly higher than those from *G. sacculifer*. Mg/Ca temperatures derived from *G. ruber* indicates that MIS 5e was warmer than the Holocene, which is also observed at a core site close to MD90-0963 [Saraswat *et al.*, 2006]. Large positive (2°C) and negative $\Delta(\text{Mg}/\text{Ca}-T)_{\text{ruber-sacc}}$ values (-2°C) are observed around 145 ka and 155 ka (MIS 6), respectively (Figure 10). Although these periods correspond to a high- and a low-productivity period, the influence of dissolution is not clear for these intervals because the offset is produced by an anomalously high *G. ruber* Mg/Ca around 145 ka and an anomalously high *G. sacculifer* Mg/Ca around 155 ka. From MIS 7 to MIS 10, *G. ruber* and *G. sacculifer* Mg/Ca temperatures are similar with small positive or negative offsets that are not clearly related to productivity changes. MIS 11 is expected to correspond to an intense long warm interglacial period because of the orbital configuration at that time. Indeed, *G. sacculifer* Mg/Ca shows a long warm interglacial with a maximal temperature attaining 29.4°C . By contrast, the maximal *G. ruber* Mg/Ca temperature during MIS 11 is only 28.3°C , which is lower than values during the Holocene, MIS 5, 7 and 9. Early MIS 11 is characterized by a low *G. ruber* weight (Figure 3a) and a high proportion of test loss (Figure 3d). Taken together, the offset during MIS 11 is due to partial dissolution of *G. ruber*.

[29] Except for the part of MIS 11 showing partial dissolution of *G. ruber*, the two studied foraminifera show highly consistent seawater temperatures, which suggest that initial temperature signals are preserved in spite of calcite dissolution. This result is consistent with EPMA observations showing preservation of Mg-rich parts, even in the case of “high PP” *G. ruber* (section 4.2). Foraminiferal test dissolution could be influenced by both chemical composition and ultrastructure of tests. Porous test structure increases surface/volume ratio facilitating calcite dissolution. SEM (Figure 4) and EPMA (Figures 5–7) observations reveal that dissolution smoothed test surface, broadened and deepened the pores. This process partially removes chamber wall but the influences on Mg-rich layers inside of the chambers seems to be small. We speculate that at the beginning of mild dissolution, modification of foraminiferal Mg/Ca is less or similar amplitude to uncertainty of temperature estimate. Our results indicate that test dissolution does not always lead to a significant reduction of foraminiferal Mg/Ca ratio.

5.3. Paleoceanographic Implications

[30] Although the results of core MD90-0963 indicate negligible effect of supralysoclinal calcite dissolution on the foraminiferal Mg/Ca thermometer, generalization of this result to the whole ocean is still premature and there exists several parameters, which should be considered. Carbonate content in sediments might be one of the most important factors to be considered. Jahnke and Jahnke [2004] have shown that, at sites where sediments contain more than 35% CaCO_3 , the carbonate dissolution rate is much lower than in low- CaCO_3 sediments. Thus, better preservation of the foraminiferal Mg/Ca signal is expected in carbonate-rich sediments. Indeed, core MD90-0963 has a carbonate content ranging between 40 and 80% for the last 460 ka [Bassinot *et al.*, 1994b]. This suggests that the distribution of sedimentary calcite content, such as obtained by calcite content mapping proposed by Archer and Maier-Reimer [1994], could provide a preliminary idea of whether foraminiferal Mg/Ca thermometry can be applied to the core site. The carbonate content in sediments is determined by the interaction between organic carbon and calcite flux ratio, calcite saturation state in bottom water and sedimentation rate. Therefore, oceanic ventilation rate and change in primary producers have a profound effect on the foraminiferal Mg/Ca signal. Another important factor is sediment compaction, which is frequently observed in the lower parts of sediment cores. This is the case for *G. ruber* dissolution during MIS 11, which is characterized by reduced test weight accompanied by high test loss.

[31] To date, there is no universal indicator of good preservation of foraminiferal Mg/Ca. The criteria may vary from site to site, and a single indicator is insufficient to monitor the possible influence of dissolution. Thus, we strongly recommend the routine analysis of a series of indicators including test weight, proportion of test loss during cleaning, foraminiferal Mn/Ca and bulk CaCO_3 content.

6. Conclusions

[32] To study the influence of supralysoclinal calcite dissolution produced by metabolic respiration on the foraminiferal Mg/Ca thermometer, we applied multiproxy approaches to a core collected from the eastern Arabian Sea covering a sedimentary record over the last 450 ka. The studied core contains 40–80% CaCO_3 and is characterized by



precession-cycled paleoproductivity changes leading to calcite dissolution. We obtained data on bulk and microscale chemical composition, narrow-sized weights and test ultrastructure for *Globigerinoides ruber* and *Globigerinoides sacculifer* in selected samples corresponding to periods of high and low productivity.

[33] For samples selected from high-productivity intervals, the test weights of both species tend to decrease with increasing foraminiferal Mn/Ca. This indicates a decrease in pH and Eh due to metabolic CO₂ release. Scanning electron microprobe analyses reveal that test ultrastructure is preserved in *G. sacculifer*, whereas it is partially degraded in *G. ruber* within the high-productivity sample. Electron probe microanalysis show that Ca content in *G. ruber* test decreases in the high-productivity sample, leading to a decrease in test density. In spite of the calcite dissolution, Mg-rich bands are preserved in *G. ruber* chamber sections, suggesting that Mg-rich parts are not always preferentially removed. Assuming that the test weight changes are produced by calcite dissolution, the estimated Mg/Ca temperature bias is of the order of 1°C on the basis of calibration equations due to *Dekens et al.* [2002] and *Rosenthal and Lohmann* [2002] and comparison between *G. ruber* and *G. sacculifer*. Despite strong evidence of test dissolution, foraminiferal Mg/Ca of both species seems to preserve the initial temperature signal under the studied conditions, except in marine isotope stage (MIS) 11 where *G. ruber* test loss by cleaning exceeds 80%.

[34] In the studied core, we find there is a negligible influence of supralysocline calcite dissolution on the foraminiferal Mg/Ca thermometer. This is consistent with the low calcite dissolution rate of sediments with high carbonate content (>35%) underlying supersaturated bottom waters [*Jahnke and Jahnke*, 2004]. However, our results do not imply that supralysocline calcite dissolution can never have any impact on foraminiferal Mg/Ca. Since there is no perfect indicator of foraminifera Mg/Ca preservation, we strongly recommend routine monitoring of a series of indicators including test weight, proportion of test loss during cleaning, foraminiferal Mn/Ca, and CaCO₃ content. Mg/Ca values are not reliable when based on samples with more than 80% test loss by cleaning.

Acknowledgments

[35] The authors thank L. Vidal for fruitful discussions during drafting of an early manuscript. F. Rostek kindly provided

unpublished alkenone concentration data. O. Grauby is thanked for help with SEM analyses and N. Buchet for some foraminifera preparation. Instructive comments made by the editor and two anonymous reviewers improved the manuscript. This work is partly financed by ANR-05-BLANC-0312-01 and KAKENHI 18740330. M.S.N. Carpenter post-edited the English style.

References

- Andrulleit, H., S. Stager, U. Rogalla, and P. Cepek (2003), Living coccolithophores in the northern Arabian Sea: Ecological tolerances and environmental control, *Mar. Micropaleontol.*, *49*(1–2), 157–181, doi:10.1016/S0377-8398(03)00049-5.
- Antoine, D., J.-M. Andre, and A. Morel (1996), Oceanic primary production: 2. Estimation at global scale from satellite (coastal zone color scanner) chlorophyll, *Global Biogeochem. Cycles*, *10*, 57–69, doi:10.1029/95GB02832.
- Archer, D., and E. Maier-Reimer (1994), Effect of deep-sea sedimentary calcite preservation on atmospheric CO₂ concentration, *Nature*, *367*, 260–264, doi:10.1038/367260a0.
- Bard, E. (2001a), Comparison of alkenone estimates with other paleotemperature proxies, *Geochem. Geophys. Geosyst.*, *2*(1), doi:10.1029/2000GC000050.
- Bard, E. (2001b), Paleooceanographic implications of the difference in deep-sea sediment mixing between large and fine particles, *Paleoceanography*, *16*(3), 235–239, doi:10.1029/2000PA000537.
- Barker, S., and H. Elderfield (2002), Foraminiferal calcification response to glacial-interglacial changes in atmospheric CO₂, *Science*, *297*, 833–836, doi:10.1126/science.1072815.
- Barker, S., M. Greaves, and H. Elderfield (2003), A study of cleaning procedures used for foraminiferal Mg/Ca paleothermometry, *Geochem. Geophys. Geosyst.*, *4*(9), 8407, doi:10.1029/2003GC000559.
- Barker, S., I. Cacho, H. M. Benway, and K. Tachikawa (2005), Planktonic foraminiferal Mg/Ca as a proxy for past oceanic temperatures: A methodological overview and data compilation for the Last Glacial Maximum, *Quat. Sci. Rev.*, *24*, 821–834, doi:10.1016/j.quascirev.2004.07.016.
- Bassinot, F., L. D. Labeyrie, E. Vincent, X. Quidelleur, N. J. Shackleton, and Y. Lancelot (1994a), The astronomical theory of climate and the age of the Brunhes-Matuyama magnetic reversal, *Earth Planet. Sci. Lett.*, *126*(1–3), 91–108, doi:10.1016/0012-821X(94)90244-5.
- Bassinot, F. C., L. Beaufort, E. Vincent, L. D. Labeyrie, F. Rostek, P. J. Müller, X. Quidelleur, and Y. Lancelot (1994b), Coarse fraction fluctuations in pelagic sediments from the tropical Indian Ocean: A 1500-kyr record of carbonate dissolution, *Paleoceanography*, *9*(4), 579–600, doi:10.1029/94PA00860.
- Bé, A. W. H., C. Hemleben, O. R. Anderson, and M. Spindler (1980), Pore structures in planktonic foraminifera, *J. Foraminiferal Res.*, *10*, 117–128.
- Beaufort, L., Y. Lancelot, P. Camberlin, O. Cayre, E. Vincent, F. Bassinot, and L. Labeyrie (1997), Insolation cycles as a major control of equatorial Indian Ocean primary production, *Science*, *278*, 1451–1454, doi:10.1126/science.278.5342.1451.
- Bijma, J., H. J. Spero, and D. W. Lea (1999), Reassessing foraminiferal stable isotope geochemistry: Impact of the oceanic carbonate system (experimental results), in *Uses of Proxies in Paleoceanography: Examples From the South Atlantic*, edited by G. Fischer and G. Wefer, pp. 489–512, Springer, Berlin.



- Broecker, W. S., and E. Clark (2001), An evaluation of Lohmann's foraminifera weight dissolution index, *Paleoceanography*, *16*, 531–534, doi:10.1029/2000PA000600.
- Brown, S. J., and H. Elderfield (1996), Variations in Mg/Ca and Sr/Ca ratios of planktonic foraminifera caused by postdepositional dissolution: Evidence of shallow Mg-dependent dissolution, *Paleoceanography*, *11*, 543–551, doi:10.1029/96PA01491.
- Cayre, O., L. Beaufort, and E. Vincent (1999), Paleoproductivity in the equatorial Indian Ocean for the last 260,000 yr: A transfer function based on planktonic foraminifera, *Quat. Sci. Rev.*, *18*, 839–857, doi:10.1016/S0277-3791(98)00036-5.
- Conkright, M., S. Levitus, T. O'Brien, T. Boyer, J. Antonov, and C. Stephens (1998), *World Ocean Atlas 1998 CD-ROM Data Set Documentation*, Tech. Rep. 15, 16 pp., Natl. Oceanogr. Data Cent., Silver Spring, Md.
- Dekens, P. S., D. W. Lea, D. K. Pak, and H. Spero (2002), Core top calibration of Mg/Ca in tropical foraminifera: Refining paleo-temperature estimation, *Geochem. Geophys. Geosyst.*, *3*(4), 1022, doi:10.1029/2001GC000200.
- de Villiers, S. (2003), A 425 kyr record of foraminiferal shell weight variability in the western equatorial Pacific, *Paleoceanography*, *18*(4), 1080, doi:10.1029/2002PA000801.
- de Villiers, S. (2004), Optimum growth conditions as opposed to calcite saturation as a control on the calcification rate and shell-weight of marine foraminifera, *Mar. Biol.*, *144*, 45–49, doi:10.1007/s00227-003-1183-8.
- de Villiers, S., M. Greaves, and H. Elderfield (2002), An intensity calibration method for the accurate determination of Mg/Ca and Sr/Ca of marine carbonates by ICP-AES, *Geochem. Geophys. Geosyst.*, *3*(1), 1001, doi:10.1029/2001GC000169.
- Dittert, N., and R. Henrich (2000), Carbonate dissolution in the South Atlantic Ocean: evidence from ultrastructure breakdown in *Globigerina* bulloides, *Deep Sea Res. Part I*, *47*, 603–620, doi:10.1016/S0967-0637(99)00069-2.
- Eggins, S. M., P. De Deckker, and J. Marchall (2003), Mg/Ca variation in planktonic foraminifera tests: implications for reconstructing palaeo-seawater temperature and habitat migration, *Earth Planet. Sci. Lett.*, *212*, 291–306, doi:10.1016/S0012-821X(03)00283-8.
- Hemleben, C., M. Spindler, and O. R. Anderson (1988), *Modern Planktonic Foraminifera*, Springer, New York.
- Jahnke, R., and D. Jahnke (2004), Calcium carbonate dissolution in deep sea sediments: Reconciling microelectrode, pore water and benthic flux chamber results, *Geochim. Cosmochim. Acta*, *68*(1), 47–59, doi:10.1016/S0016-7037(03)00260-6.
- Kawahata, H., A. Nishimura, and M. K. Gagan (2002), Seasonal change in foraminiferal production in the western equatorial Pacific warm pool: Evidence from sediment trap experiments, *Deep Sea Res. Part II*, *49*, 2783–2800, doi:10.1016/S0967-0645(02)00058-9.
- Lea, D. W. (2004), The 100 000-yr cycle in tropical SST, greenhouse forcing, and climate sensitivity, *J. Clim.*, *17*, 2170–2179, doi:10.1175/1520-0442(2004)017<2170:TYCITS>2.0.CO;2.
- Lea, D. W., D. K. Pak, and H. J. Spero (2000), Climate impact of late Quaternary equatorial Pacific sea surface temperature variations, *Science*, *289*, 1719–1724, doi:10.1126/science.289.5485.1719.
- Lewis, E., and D. Wallace (2000), Program developed for CO₂ system calculations, *ORNL/CDIAC-105*, Carbon Dioxide Inf. Anal. Cent., Oak Ridge Natl. Lab., U.S. Dep. of Energy Oak Ridge, Tenn. (Available at <http://cdiac.esd.ornl.gov/oceans/co2rprt.html>)
- Mashiotta, T. A., D. W. Lea, and H. J. Spero (1999), Glacial-interglacial changes in Subantarctic sea surface temperature and $\delta^{18}\text{O}$ -water using foraminiferal Mg, *Earth Planet. Sci. Lett.*, *170*, 417–432, doi:10.1016/S0012-821X(99)00116-8.
- Muller, P. J., M. Cepek, G. Ruhland, and R. R. Schneider (1997), Alkenone and coccolithophorid species changes in late Quaternary sediments from the Walvis Ridge: Implications for the alkenone paleotemperature method, *Palaeogeogr. Palaeoclimatol. Palaeoecol.*, *135*(1–4), 71–96, doi:10.1016/S0031-0182(97)00018-7.
- Nürnberg, D. (2000), Taking the temperature of past ocean surfaces, *Science*, *289*, 1698–1699, doi:10.1126/science.289.5485.1698.
- Okai, T., A. Suzuki, H. Kawahata, S. Terashima, and N. Imai (2001), Preparation of a new Geological Survey of Japan geochemical reference material: Coral JCp-1, Geostand, *Geoanal. Res.*, *26*(1), 95–99, doi:10.1111/j.1751-908X.2002.tb00627.x.
- Pailler, D., E. Bard, F. Rostek, Y. Zheng, R. Mortlock, and A. Van Geen (2002), Burial of redox-sensitive metals and organic matter in the equatorial Indian Ocean linked to precession, *Geochim. Cosmochim. Acta*, *66*(5), 849–865, doi:10.1016/S0016-7037(01)00817-1.
- Rosenthal, Y., and G. P. Lohmann (2002), Accurate estimation of sea surface temperature using dissolution-corrected calibration for Mg/Ca, *Paleoceanography*, *17*(3), 1044, doi:10.1029/2001PA000749.
- Rosenthal, Y., G. P. Lohmann, K. C. Lohmann, and R. M. Sherrell (2000), Incorporation and preservation of Mg in *Globigerinoides sacculifer*: Implication for reconstructing the temperature and $^{18}\text{O}/^{16}\text{O}$ of seawater, *Paleoceanography*, *15*, 135–145, doi:10.1029/1999PA000415.
- Rosenthal, Y., et al. (2004), Interlaboratory comparison study of Mg/Ca and Sr/Ca measurements in planktonic foraminifera for paleoceanographic research, *Geochem. Geophys. Geosyst.*, *5*, Q04D09, doi:10.1029/2003GC000650.
- Rostek, F. G., G. Ruhland, F. C. Bassinot, P. J. Müller, L. D. Labeyrie, Y. Lancelot, and E. Bard (1993), Reconstructing sea surface temperature and salinity using $\delta^{18}\text{O}$ and alkenone records, *Nature*, *364*, 319–321, doi:10.1038/364319a0.
- Rostek, F., G. Ruhland, F. C. Bassinot, L. Beaufort, P. J. Muller, and E. Bard (1994), Fluctuations of the Indian monsoon regime during the last 170,000 years: Evidence from sea surface temperature, and salinity and organic carbon records, in *Global Precipitations and Climate Change*, edited by M. Besbois and F. Desalmand, pp. 27–51, Springer, Heidelberg.
- Rostek, F., E. Bard, L. Beaufort, C. Sonzogni, and G. Ganssen (1997), Sea surface temperature and productivity records for the past 240 kyr in the Arabian Sea, *Deep Sea Res. Part II*, *44*, 1461–1480, doi:10.1016/S0967-0645(97)00008-8.
- Russell, A., S. Emerson, B. K. Nelson, J. Erez, and D. W. Lea (1994), Uranium in foraminiferal calcite as a recorder of seawater uranium concentrations, *Geochim. Cosmochim. Acta*, *58*, 671–681, doi:10.1016/0016-7037(94)90497-9.
- Russell, A., B. Honisch, H. J. Spero, and D. W. Lea (2004), Effects of seawater carbonate ion concentration and temperature on shell U, Mg, and Sr in cultured planktonic foraminifera, *Geochim. Cosmochim. Acta*, *68*, 4347–4361, doi:10.1016/j.gca.2004.03.013.
- Sadekov, A. Y., S. M. Eggins, and P. De Deckker (2005), Characterization of Mg/Ca distributions in planktonic foraminifera species by electron microprobe mapping, *Geochem. Geophys. Geosyst.*, *6*, Q12P06, doi:10.1029/2005GC000973.
- Saraswat, R., R. Nigam, S. Weldeab, A. Mackensen, and P. D. Naidu (2006), A first look at past sea surface temperatures in the equatorial Indian Ocean from Mg/Ca in foraminifera, *Geophys. Res. Lett.*, *32*, L24605, doi:10.1029/2005GL024093.



Schulte, S., and E. Bard (2003), Past changes in biologically mediated dissolution of calcite above the chemical lysocline recorded in Indian Ocean sediments, *Quat. Sci. Rev.*, 22, 1757–1770, doi:10.1016/S0277-3791(03)00172-0.

Schulte, S., F. Rostek, E. Bard, J. Rullkötter, and O. Marechal (1999), Variations of oxygen-minimum and primary productivity recorded in sediments of the Arabian Sea, *Earth Planet. Sci. Lett.*, 173, 205–221, doi:10.1016/S0012-821X(99)00232-0.